Characterization of Polymer Morphology in Polyurethane Foams Using Atomic Force Microscopy

Qiang Lan,[1] Greg Haugstad[2]

[1]Huntsman Polyurethanes, 8600 Gosling Road, The Woodlands, Texas 77381
[2]Characterization Facility, University of Minnesota, 12 Shepherd Labs, Minneapolis, Minnesota 55455

ABSTRACT: One of the most important challenges in polyurethane (PU) science is characterization of foam morphologies, which provides information to help understand material properties and improve synthesis conditions. Atomic force microscopy (AFM) is a very useful technique to obtain such information. A key challenge is to apply this technique to PU foams without destroying their cell structure. In this article, we describe the development of a methodology to characterize different types of PU foams using AFM while keeping the foam cells intact. Epoxy resin was used to impregnate the foams and was cured afterwards. Smooth surfaces were created using a micro-tome to minimize topographic effects during AFM examination. Phase information was obtained on the PU matrix and differentiated from the epoxy in AFM. This technique is demonstrated using several different foams including a flexible foam, two different elastomeric foams, and a rigid foam nanocomposite. Comparison with compression techniques reveals that the proposed method does not modify foam morphology. © 2011 Wiley Periodicals, Inc. J Appl Polym Sci 121: 2644–2651, 2011

Key words: atomic force microscopy; polyurethanes; foams; morphology

INTRODUCTION

Polyurethanes (PU) have been finding use in a growing number of applications in many industries (such as furniture, construction, footwear, and automotive) for decades, making them the most versatile plastic materials. The majority of PUs have been applied as cellular materials, for instance, flexible foams providing enjoyable comfort for mattresses and seating, and rigid foams for excellent thermal insulation in appliance and construction applications. Most PU foams are manufactured by a one-shot process, where the polymer matrix is formed by urethane and urea reaction, and simultaneously blown by physical blowing agent with low boiling point and/or by chemical reaction such as water-isocyanate reaction releasing carbon dioxide. The reaction between water and isocyanate is of particular importance for PU flexible foams,[1] because (1) it is the main blowing mechanism for current flexible foam technology, and (2) the urea formation due to the water-isocyanate reaction plays a vital role in forming the open-cell structure and the macro-/

microphase separated morphology of polymer matrix. Because of strong hydrogen bonding, the urea structure can easily aggregate in various sizes and separate from the soft domain derived mainly from high-molecular weight polyols. Microphase separated urea domains act as physical crosslinks contributing to load-bearing properties, while macrophase separated urea domains or so-called urea balls help to induce cell opening by promoting the rupture of cell windows.[1] The complicated morphologies of polymer matrix can be controlled by the balance between the water-isocyanate reaction and polyol-isocyanate reaction, and by the compatibility between various structures formed during reaction. Similar morphologies have also been observed for elastomeric foams in, for example, footwear applications, where most of water is usually replaced by chain extenders to increase the overall foam density. Most recently, polyurethane nanocomposites have introduced new features in PU foams. It is important in this case to understand the relationship between the nanoparticles and the morphology of the foam.

The properties of PU foams are determined by cellular structure and morphology of polyurethane polymer. There has been no universal technique yet to characterize both cellular structure and polymer morphology at the same time. The cell structure including cell size and distribution, and cell orientation is typically examined by scanning electron microscope (SEM) and optical microscope,[2,3] while

PU morphology has to be characterized by other techniques. Transmission electron microscopy (TEM) has been used to image the urea balls in flexible foams.[4–6] It is very difficult, however, to image the rigid microdomains using only the intrinsic mass difference (thickness and density) between rigid and soft domains. Staining techniques can be applied to enhance contrast, but these are often ineffective in polyurethanes. Small angle X-ray scattering (SAXS) also has been used to characterize the microphase segregation, interdomain spacing, and interface thickness in polyurethanes.[4–6] However, SAXS does not provide direct information on domain size distribution and connectivity. There is also a practical limit on the measurement of large domains (hundreds of nanometers and even microns), which exist in PU materials. Sometimes, the interpretation of the data relies heavily on mathematical models,[7] which is difficult to establish for complex morphologies observed in polyurethanes.

More recently, atomic force microscopy (AFM) has been applied to image the phase structure of polyurethanes.[8,9] In contrary to TEM, no staining is required. In the widely used dynamic AFM mode operated in intermittent contact (a.k.a. "tapping mode"), sufficient contrast between soft and rigid domains can be created from the difference in stiffness and tip-sample adhesion. The largest domain size that can be imaged is only limited by the scan size, which can be as large as 100 μm × 100 μm. On the low end of the scale, on the other hand, AFM allows one to study features in the nanometer range. Different types of polyurethane materials can be characterized by AFM. For the water blown flexible slabstock foams, Kaushiva et al.[10] revealed lamellar-like urea rigid domains in a typical formulation system using AFM. The foams were mechanically compressed or crushed. They suspected that the urea balls are the clusters of such lamellae. They also studied the connectivity of the urea rigid domains as the concentration reached a certain limit.[11] They found that diethanol amine can disrupt such connectivity. Rightor et al.[12] used a combination of X-ray spectroscopy and AFM to examine the detailed structure of urea rich domains on polyurethane plaques. AFM bolstered the conclusion of Li et al.[13] from SAXS that the mechanism of the phase segregation of urea domains was spinodal decomposition and the structure was bicontinuous. Polymer nanocomposites,[14,15] including polyurethane foam nanocomposites,[16,17] have attracted intense research interest in recent years and provide another useful field of application for AFM. One important issue for polymer nanocomposites is how to disperse well the nanoparticles and control their location in the foam structure (i.e., foam windows versus struts). TEM has been useful to obtain such structural informa-

tion. AFM also can be applied for this purpose with certain advantages. Although AFM has been demonstrated to be a powerful technique to investigate the morphology in PU materials, AFM scanning requires a relatively smooth solid surface which is not the case for PU foams. As reported previously, AFM samples had to be prepared into dense solids by either collapsing the foam during synthesis[18] or compressing the foam after foaming.[19] These sample preparations destroy the cellular structure of PU foams, making it impossible to characterize the PU morphology in a particular cell configuration such as cell strut and cell window. Identifying these features is essential to understand the mechanism of cell opening and various properties of final foam products. The compressing method involves applying a compressive stress at high temperatures; this procedure might also impact the PU morphology.

In this study, we describe the development of a methodology to image the foam cells by impregnating the PU foams with epoxy, curing the epoxy, performing microtomy and finally imaging with AFM. Using this novel methodology, the phase morphology can be obtained with the foam cells intact. Phase structure is compared with AFM images of compressed PU foams to demonstrate the advantages of this new sample preparation technique. This method is further extended to investigate the distribution of nanoparticles in closed-cell PU rigid foams.

EXPERIMENTAL

Foam preparation

Two water blown elastomer foams, A and B, were prepared using a mixture of 1,4-butane diol (Sigma Aldrich) and either JEFFOL® G31-28 polyether polyol (foam A) or DALTOCEL® F-555 polyether polyol (foam B) with DABCO® S-25 amine catalyst (Air Products). The blends were reacted with SUPRA-SEC® 2433 MDI prepolymer from Huntsman International LLC. Both elastomer foams possess 34% rigid block content. The foam density is approximately 0.21 g/cm³. A flexible foam C was prepared from polyether polyols (copolymers of propylene oxide, PO, and ethylene oxide, EO). Standard surfactants and catalysts were used. The isocyanate is MDI based. Water was the sole blowing agent. The density of the foam C is about 0.036 g/cm³. A rigid foam nanocomposite, D, was prepared from JEFFOL SD-361 polyether polyol and RUBINATE® M, polymeric MDI, from Huntsman. JEFFCAT® ZF-22 tertiary amine catalyst, JEFFCAT PMDETA tertiary amine catalyst and JEFFCAT DMCHA tertiary amine catalyst from Huntsman International LLC were used in a mixture to catalyze this reaction. A typical silicone catalyst, NIAX® L-6900 (Momentive

Performance Materials) was also used. HCFC-141b (A-Gas Inc.) was used as blowing agent. The foam also contained tris(2-chloro-1-methylethyl) phosphate (Sigma Aldrich). Proprietary alumina nanoparticles (32 nm in diameter) were introduced as fillers in the rigid foam. The density of foam D is 0.033 g/cm^3. General formulation principles for these foams can be found elsewhere.[20]

All foams were prepared in a similar way. The ingredients except isocyanate were premixed into a blend which was mixed with isocyanate using a blade at 2000 rpm for 10 s. The mixture was then poured into a paper cup to prepare free rise foams. For rigid foam nanocomposite D, the alumina nanoparticles were dispersed in polyol first using sonication, followed by the same procedure described above to prepare the foam.

Scanning electron microscopy characterization

The elastomer foams were fractured in liquid nitrogen. The fracture surface (coated with 3 nm thick Pt) was examined using a Hitachi S-4700 cold field emission SEM with secondary electron detector operated at a low acceleration voltage of 3 keV and a low emission current of 10 μA.

Atomic force microscopy characterization

Phase imaging in dynamic AFM was used to image the polyurethane foams. The phase lag relates to the energy dissipation during tip-sample interaction,[21] and is imaged to provide materials contrast. Property variations across the surface, such as those due to differences in (visco)elastic character and/or tip-sample adhesion, can create contrast in phase images. AFM experiments were conducted on a Digital Instruments Nanoscope III Multimode in ambient conditions. The drive amplitude and drive frequency were adjusted to place the system in the repulsive or intermittent-contact regime (true "tapping") as diagnosed with the phase signal.[22] The drive frequency was set about 0.2 kHz below resonance and the free-oscillation amplitude was 30–45 nm. Usually the set point amplitude ratio (operational amplitude to free amplitude) was fixed around 0.9. The scan rate was 1 Hz. Nano World Arrow^{TM} NC probes were used for the imaging. The force constant is 27–80 N/m, and the resonance frequency was about 285 kHz.

AFM specimen preparation

All the ingredients of the epoxy (low viscosity "spur" kit from Ted Pella) were mixed thoroughly at room temperature. Small pieces of the foams (about 10 mm × 3 mm × 3 mm) were put in silicone rubber

molds before they were filled with the epoxy liquid. The molds were moved to a vacuum dessicator, and low vacuum was applied to remove the air inside the foams without boiling the epoxy liquid. After most of the air in the foams was removed, the molds were transferred to an oven which was preheated to 60°C. The epoxy was cured for 24 h. The impregnated PU foams were microtomed to create smooth cross-section surfaces at −124°C for elastomer and flexible foams, and at room temperature for the rigid foam nanocomposite.

RESULTS AND DISCUSSIONS

Before the results obtained using this epoxy-impregnation method are presented, the elastomeric foams A and B imaged with AFM, after compressed at 160°C for 10 min to remove the cell structure, are shown in Figure 1. The formulations for A and B are the same except that the polyol in foam A possesses a lower EO/PO ratio than the polyol in foam B. The brighter domains of the phase images are assigned to relatively rigid, isocyanate-rich domains in the elastomers, because of the expected lesser energy dissipation under tip-sample interaction, in turn related to greater rigidity and lesser tip-sample adhesion. The dark domains are thus assigned to polyol rich regions.

We note that Sonnenschein et al.[23] used RuO$_4$ to stain polyurethane foams before AFM imaging, probably to enhance the contrast. Consistent with our results, it has been demonstrated[24] that staining is not generally necessary to achieve adequate phase contrast in polyurethanes.

From the phase image in Figure 1(a), the domain size in foam A is micron scale. In some areas, the soft domains are lower in height than the rigid domains. This may arise from differential relaxation during warm-up from approximately −120°C following cryo-microtomy. However, clearly the starkest differentiation of the phase segregation is indeed provided by the phase image, in turn related to tip-sample energy dissipation. This image suggests that there is stretching of domains in Foam A (the arrow in the phase image indicates the elongation direction). By direct section measurement in NanoScope software, the average width and length of elongated rigid domains is estimated to be about 0.8 μm and >5.4 μm respectively. So the aspect ratio is estimated close to 7. Of course a more accurate result for the whole sample requires similar analysis on many more such images. We hypothesize that this anisotropic domain is due to mechanical compression during sample preparation. For foam B shown in Figure 1(b,c), the phase domain size looks much smaller. The domain shapes are irregular. A power spectral density analysis (PSD) is used to estimate
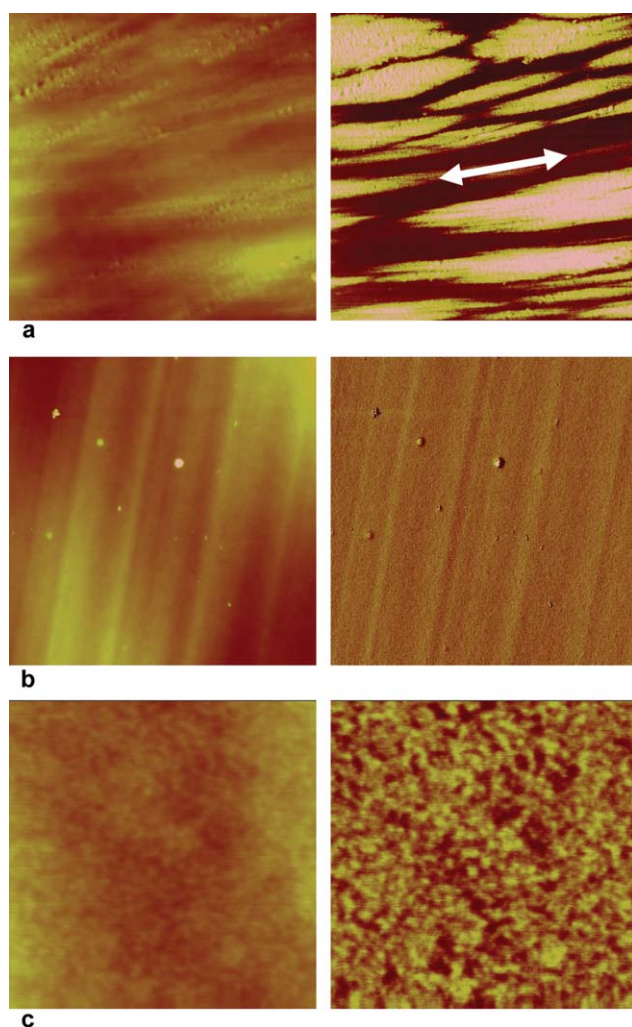
Figure 1 (a) Elastomer foam A. Left: height image. Right: phase image. The scan size is 10 μm × 10 μm. (b) Elastomer foam B. Left: height image. Right: phase image. The scan size is 10 μm × 10 μm. (c) Elastomer foam B. Left: height image. Right: phase image. The scan size is 500 nm × 500 nm. [Color figure can be viewed in the online issue, which is available at wileyonlinelibrary.com]

the dominant periodic structure in the phase image in Figure 1(c). The estimated domain period is in the range of 33–63 nm, which is indeed much smaller, in nanoscale. No obvious stretching of domains in Foam B is observed, which is probably due to the smaller size of phase segregation. Different polyol chain compositions (EO/PO ratio) lead to significantly different phase size and shape due to different interaction parameters with rigid block, which actually contributes to the different mechanical properties of the foams. This structure–property relationship is not the focus of this manuscript and will not be further discussed. However, the importance of phase structure, as revealed by AFM, is clearly illustrated.

Obviously, no cells exist after the foams are compressed. To preserve the cell structure and analyze

the morphology of cell strut/junction, both elastomeric foams were also impregnated with epoxy and examined using AFM.
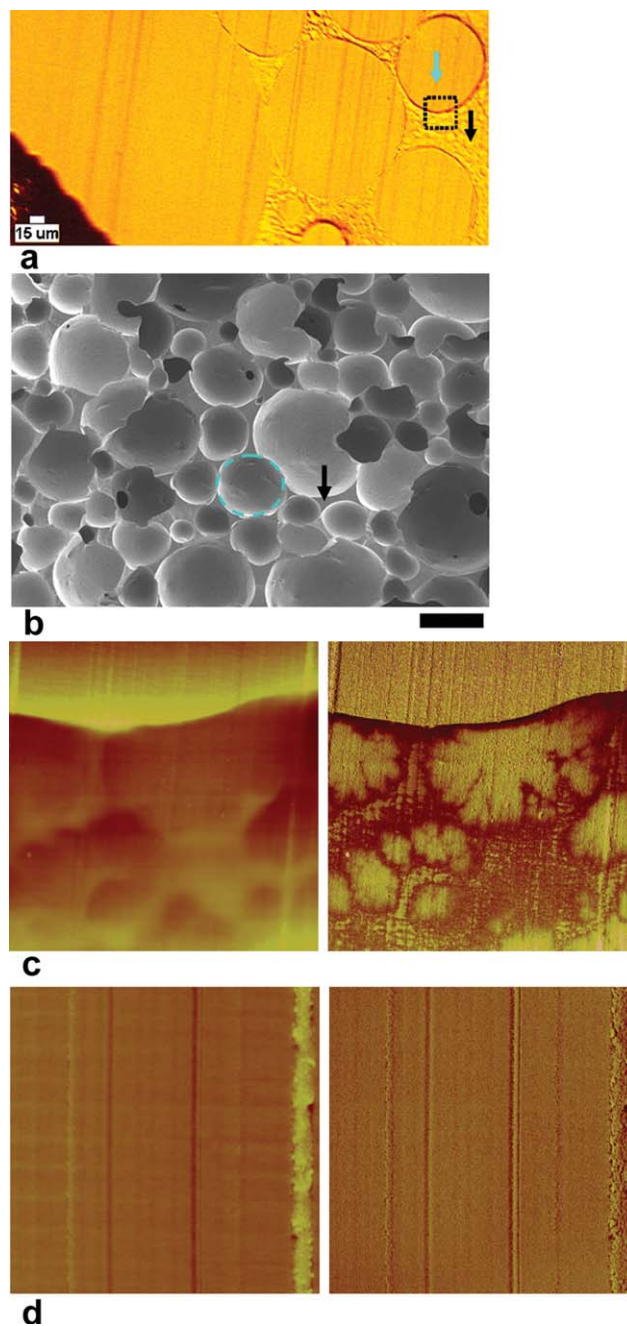

Figure 2 (a) Optical microscopy of a cross section of epoxy-impregnated foam A. The square frame indicates the interface area scanned. The black arrow indicates the PU and the blue arrow indicates the epoxy. (b) Secondary electron SEM image of fracture surface of foam A before impregnated with epoxy. The scale bar is 150 μm. (c) Height (left) and phase (right) images of the interface. The scan size is 15 μm × 15 μm. (d) Height (left) and phase (right) images of the epoxy indicated by the blue arrow in (a). The scan size is 3 μm × 3 μm. [Color figure can be viewed in the online issue, which is available at wileyonlinelibrary.com]
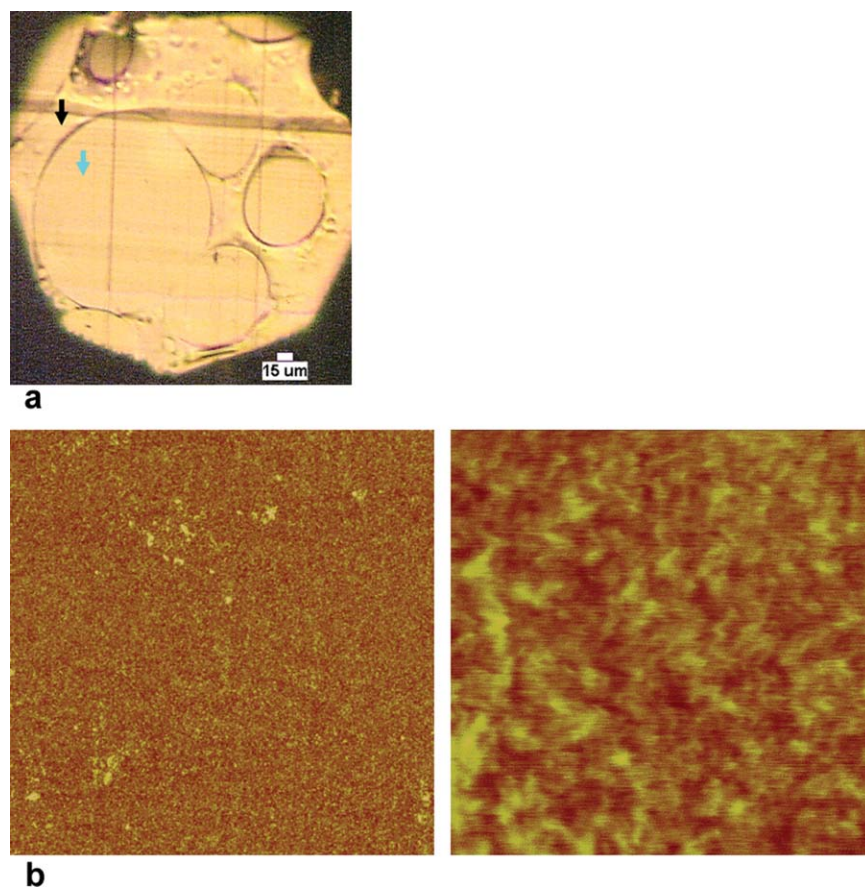
Figure 3 (a) Optical microscope image of a cross section of the epoxy impregnated foam B. The black arrow indicates the PU and the blue arrow indicates the epoxy. (b) Phase images of the foam B indicated by the black arrow in (a). The scan size is 5 μm × 5 μm for the left image and 500 nm × 500 nm for the right image. [Color figure can be viewed in the online issue, which is available at wileyonlinelibrary.com]

The microtomed surface of foam A impregnated with epoxy is shown in Figure 2(a) along with a SEM image in Figure 2(b) of fractured surface before epoxy impregnation. Two types of areas with distinct interface are observed in the optical micrograph of Figure 2(a), which are indicated by the black and blue arrows. The overall topography of foam fracture surface in the SEM image indicates the inherent difficulty in preparing a flat region for AFM imaging, in the absence of sample processing. The foam cells generally possess spherical shape, indicate by the blue circle. The cell strut is indicated by the black arrow. Assuming the epoxy fills open cells, the regions should appear roughly circular. So by comparing the optical micrograph and the SEM image, the circular domains (blue arrow) in Figure 2(a) are expected to be epoxy whereas the domain indicated by the black arrow is then the polyurethane. The contrast of secondary electron imaging in Figure 2(b) is topographic contrast.[25] Although backscattering electron imaging provides compositional (atomic number) contrast,[25] it cannot be applied to image the phase structure of polyurethanes due to similar atomic composition in both soft and rigid domains

(C, H, O). The optical microscope does not possess the capability of imaging the phase structure either. To analyze the phase morphology, the dashed square subregion in Figure 2(a) was examined with AFM, shown in Figure 2(c). In the phase image, the epoxy part in the top portion appears generally brighter and more uniform than the polyurethane in the bottom portion, consistent with the epoxy being stiffer and thus less lossy than the polyurethane elastomer. In the bottom portion, the multiphase structure with micron-scale, rigid subdomains is consistent with the general morphology in Figure 1(a), but *without the distortions*: there is no identifiable stretching or elongation of the domains along any direction. By directly measuring the size of the rigid domains in Figure 2(c), the aspect ratio is estimated ~1.3 [compare with ~7 in Fig. 1(a)]. This confirms the preceding hypothesis of stretching of the domains in Foam A in Figure 1(a) due to mechanical compression during sample processing. It was observed that the volume of epoxy was slightly decreased after complete curing, which may produce interface stress. However, no obvious deformation of polyurethane solid in the foam was observed under
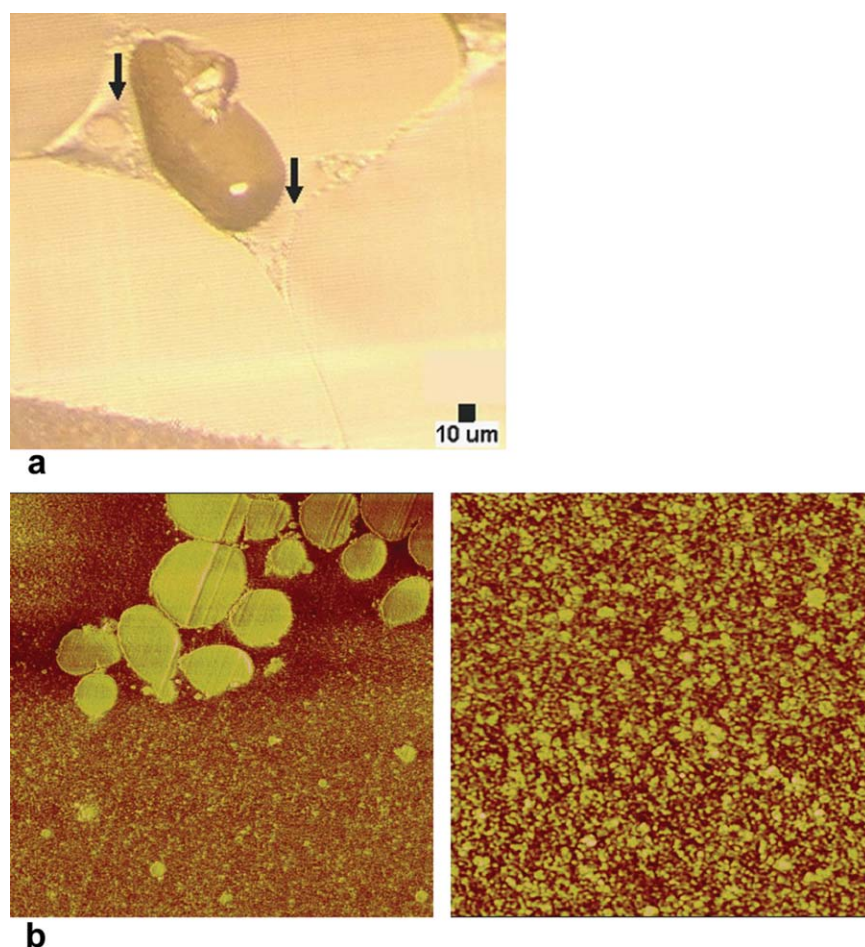
Figure 4 (a) Optical microscope image of a cross section of the epoxy impregnated flexible foam C. The arrows indicate the PU. (b) Phase images of the flexible foam C. The scan size is 10 μm × 10 μm for the left image and 3 μm × 3 μm for the right image. [Color figure can be viewed in the online issue, which is available at wileyonlinelibrary.com]

optical microscope. So it is expected that the domain shape is not significantly changed from the stress. To minimize this stress, epoxy resin with low adhesion to polyurethane is preferred. It seems that the soft domain forms a continuous phase with rigid domains dispersed in it, which is likely due to the 34% rigid block content in the elastomer. A higher magnification image of the epoxy is shown in Figure 2(d). No obvious phase segregation is observed, only linear topographic structures derived from the directionality of the microtome.

The polyurethane portion of epoxy-impregnated foam B was similarly analyzed. In the optical micrograph of Figure 3(a), the black arrow indicates the polyurethane domain imaged with AFM. Two phase images with different scan size in Figure 3(b) show, firstly, that the microphase structure is much more uniform in foam B compared to foam A, consistent with the comparison of Figure 1(a,b); secondly, that the nanophase structure is consistent with Figure 1(c). A similar PSD analysis of the 500 nm × 500 nm phase image provides the domain period about 56–100 nm, which is in a similar range of nanoscale but

different from the analysis result based on Figure 1(c). It is well known that the molecular weight and domain size distribution of commercial polyurethane elastomers, which the formulation of foam A and B is based on, is much broader than, for example, diblock copolymer with narrow molecular weight distribution. So it is not surprising that a statistical analysis result of one 500 nm × 500 nm region is different from another. On the other hand, compression at high temperature may also contribute to this difference. The less lossy, relatively rigid domains appear to be the minority phase, consistent with its 34% content of the total.

This method can be applied to characterize flexible foams as well, but without being limited to a plaque sample,[12] or crushing the foams.[26] As an example, flexible foam C was examined with dynamic AFM. The arrows in Figure 4(a), an optical microscope image of foam C in epoxy, indicate the PU foam struts. Corresponding phase images in Figure 4(b) clearly reveal microphase segregation. In some areas, bright circular domains of variable diameter from about 360 to 2000 nm are also observed, which
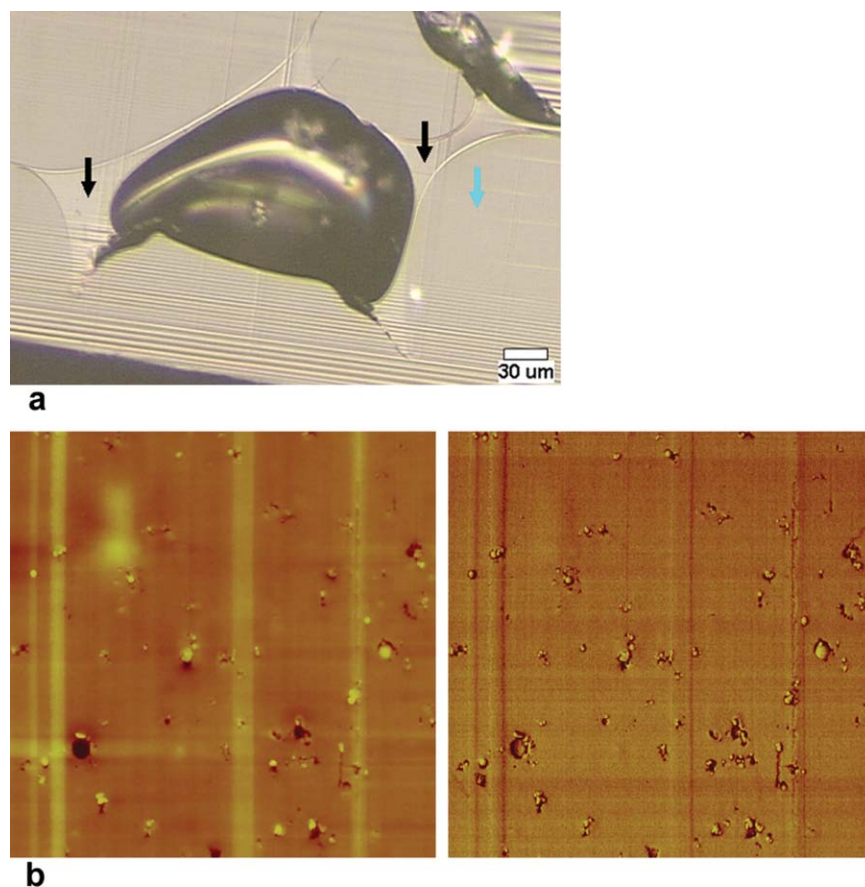
Figure 5 (a) Optical microscope image of a cross section of the epoxy impregnated rigid foam-nanoparticle composite. The black and blue arrows indicate the PU composite and the epoxy respectively. (b) Height (left) and phase (right) images of the PU composite. The scan size is 3 μm × 3 μm. [Color figure can be viewed in the online issue, which is available at wileyonlinelibrary.com]

should be polyurea rich, whether they are urea balls requires further investigation. However, the identification of such large scale domains certainly provides more information to understand the structure–property relationship in polyurethane flexible foams. The cells of the foam remain intact in the epoxy. One can image other areas such as cell junctions to reveal and compare the phase morphology. The epoxy part was also examined using dynamic AFM (not shown), possessing structures similar to that in Figure 2(d).

The rigid foam-inorganic nanoparticle composite D was processed and imaged in a similar fashion. Rigid polyurethane foams, unlike elastomer or flexible foams possess a high content of closed cells. To achieve the best filling of cells with epoxy, very thin slices (1mm or thinner) were used. After cut into a thin slice, some of the close cells were open and accessible to epoxy liquid. A flat surface is created and the polyurethane part is identified, by the black arrows in Figure 5(a). The circular features seen in both height and phase images in Figure 5(b) are the inorganic nanoparticles. In the height image, many nanoparticles protrude (appear higher than the sur-

rounding matrix) while some holes are also observed, which are believed to be due to the removal of the particles during microtomy. In the phase image, the nanoparticles generally look brighter, which is consistent with a less mechanically lossy behavior compared to the polymer. The dispersion of the particles is quite uniform, mostly in the form of small clusters as well as single particles. To quantify the dispersion of the spherical nanoparticles, one possible scenario is the average number of particles per cluster, which is based on the rationality that more uniform dispersion leads to smaller cluster and all single particles represent the best dispersion. By direct measuring, the average maximum diameter of the cluster in Figure 5(b) is estimated about 134 nm corresponding to 4.2 particles per cluster (nanoparticle diameter 32 nm), which indicates a reasonably uniform dispersion. Other scenarios to quantify the dispersion, such as the average distance between the clusters, will not be further explored. However, AFM identifies the particles at or close to the cut sample surface while TEM projects through the bulk of a thin film sample. So only when a sufficient number of cut sample surfaces are surveyed, the overall particle dispersion in the

polymer can be more accurately evaluated with AFM. If the sample is carefully microtomed and examined to identify the cell windows, potentially the locations of the particles (cell struts versus cell windows) can be characterized as well; this is a more difficult task with TEM. Such information is critical to improving properties of foams using nanoparticles (e.g., mechanical, barrier properties). Observing the phase image in Figure 5(b), the matrix does not display obvious micro-phase segregation; this is presently due to the low molecular weight and higher functionality of the components used in the foam synthesis.

CONCLUSIONS

A methodology has been developed to characterize the phase structure of the polymer in polyurethane foams with the cells intact. Dynamic AFM in the repulsive interaction regime (intermittent-contact or "tapping"/AC mode) has been used to locate the polyurethane and image the phase structure. Flexible, elastomer and rigid composite foams have been successfully characterized using this method.

References

1. Artavia, L. D.; Macosko, C. W. In Low Density Cellular Plastics: Physical Basis of Behavior; Hilyard, N. C.; Cunningham, A., Eds.; Chapman & Hall: London, 1994; Chapter 2, 22.
2. Rhodes, M.B. In Low Density Cellular Plastics: Physical Basis of Behavior; Hilyard, N. C.; Cunningham, A., Eds.; Chapman & Hall: London, 1994; Chapter 3, 56.
3. Chian, K. S.; Gan, L. H. J Appl Polym Sci 1998, 68, 509.
4. Herrington, R. M.; Turner, R. B. 1992. In Advances in Urethane Science and Technology; Frisch, K. C.; Klempner, D., Eds.; Technomic Publishing: Lancaster, Pennsylvania, 1992; Vol.11, p 1.
5. Priester, R. D., Jr.; Turner, R. B. 1994. In Low Density Cellular Plastics: Physical Basis of Behavior; Hilyard, N. C.; Cunningham, A., Eds.; Chapman & Hall: London, 1994; Chapter 4, 78.
6. Moreland, J. C.; Wilkes, G. L.; Turner, R. B.; Rightor, E. G. J Appl Polym Sci 1994, 52, 1459.
7. Visser, S. A.; Cooper, S. L. Macromolecules 1991, 24, 2584.
8. Aneja, A.; Wilkes, G. L. Polymer 2002, 43, 5551.
9. Aneja, A.; Wilkes, G. L. Polymer 2003, 44, 7221.
10. Kaushiva, B. D.; Wilkes, G. L. Polymer 2000, 41, 6987.
11. Kaushiva, B. D.; Wilkes, G. L. Polymer 2000, 41, 6981.
12. Rightor, E. G.; Urquhart, S. G.; Hitchcock, A. P.; Ade, H.; Smith, A. P.; Mitchell, G. E.; Priester, R. D.; Aneja, A.; Appel, G.; Wilkes, G. L.; Lidy, W. E. Macromolecules 2002, 35, 5873.
13. Li, W.; Ryan, A. J.; Meier, I. K. Macromolecules 2002, 35, 5034.
14. Kumar, A. P.; Depan, D.; Tomer, N. S.; Singh, R. P. Progr Polym Sci 2009, 34, 479.
15. Pavlidou, S.; Papaspyrides, C. D. Progr Polym Sci 2008, 33, 1119.
16. Cao, X.; Lee, J.; Widya, T.; Macosko, C. W. Polymer 2005, 46, 775.
17. Woo, T.; Halley, P.; Martin, D.; Kim, D. S. J Appl Polym Sci 2006, 102, 2894.
18. Aneja, A. Structure-property relationships of flexible polyurethane foams. Ph.D. thesis. Virginia Polytechnic Institute and State University: Blacksburg, VA, 2002.
19. Zhang, L.; Jeon, H. K.; Malsam, J.; Herrington, R.; Macosko, C. W. Polymer 2007, 48, 6656.
20. Randall, D.; Lee, S., Eds. The Polyurethane Book; Wiley: UK, 2002.
21. Cleveland, J. P.; Anczykowski, B.; Schmid, A. E.; Elings, V. B. Appl Phys Lett 1998, 72, 2613.
22. Haugstad, G.; Jones, R. R. Ultramicroscopy 1999, 76, 77.
23. Sonnenschein, M.; Wendt, B. J.; Schrock, A. K.; Sonney, J. M.; Ryan, A. J. Polymer 2008, 49, 934.
24. Aneja, A.; Wilkes, G. L. J Appl Polym Sci 2002, 85, 2956.
25. Goldstein, J.; Newbury, D. E.; Echlin, P.; Joy, D. C.; Roming, A. D.; Lyman, C. E.; Fiori, C.; Lifshin, E. Scanning Electron Micrscopy and X-ray Microanalysis; Plenum Press: New York, 1992.
26. Aneja, A.; Wilkes, G. L. Polymer 2004, 45, 927.